Journal of Petroleum Science and Technology 13(4): 40, 2023, Pages 2-16
DOI:10.22078/jpst.2024.4785.1798

Journal of Petroleum Science and Technology
Research Paper
https://jpst.ripi.ir/

Micropore Characteristics of Continental Shale in the Shan 1 Member of the Shanxi Formation and Controls on Gas Content: A Case Study of Well Quan 56, Yan'an Area

Zhao Weiwei*[1,2], YangDi[1], Shan Changan[1,2], Wang Fengqin[1,2] Sun Jianbo[3], Dang Wei[1,2] Duan Yifei[1], LI Fukang[3] and Yang Tianxiang[1]

1. School of Earth Sciences and Engineering, Xi'an Shiyou University, Xi'an, Shaanxi, China

2. Shaanxi Key Laboratory of Petroleum Accumulation Geology, Xi'an Shiyou University, Xi'an, Shaanxi, China

3. Research Institute of Petroleum Exploration and Development, Shaanxi Yanchang Petroleum (Group) Company Limited, Xi'an, Shaanxi, China

Abstract

The continental shale with favorable geological conditions for shale gas accumulation and broad resource prospects is widely distributed in the Ordos Basin. The micropore characteristics and controls on the gas content of Shan 1 member shale reservoir were analyzed by Argon Ion Polishing-Field Emission Scanning Electron Microscopy and Nitrogen Adsorption and High-Pressure Methane Isothermal Adsorption. The results show that the shale pore types of the Shan 1 member are primarily intergranular pores and clay mineral intergranular pores, followed by micro-fractures, dissolution pores, and organic matter pores. Different pore types provide practical storage space for shale gas. The pore size distribution of the mud shale in the Shan 1 member was strongly heterogeneous. The total pore size distribution was primarily mesoporous. Mesopores account for the most pore volume, followed by macropores and micropores, which account for the total specific surface area; macropores contribute the least specific surface area. At 90 °C, the maximum adsorption capacity of methane in mud shale was 9.02~13.02 m^3/t (average of 10.824 m^3/t). The organic carbon content in mud shale is generally low, and the organic matter pores are relatively limited. The clay mineral pores provide important specific surface and adsorption points for methane and increased gas storage capacity. The pore network system of the shale changed from inorganic to organic with increasing degrees of thermal evolution, enhancing absorbability. The differences in pore structure characteristics in the continental shale provide reliable geological accordance for revealing the difference in gas content in the Yan'an area.

Keywords: Continental Mud Shale; Pore Type; Pore Structure; Methane Sorption; Shan 1 Member; Yan'an Area; Ordos Basin.

Introduction

The Ordos Basin contains several sets of shale layers that are potential shale gas formations. Yanchang Petroleum Group achieved a breakthrough in the Chang 7 member of the shale interval of the Mesozoic era Yanchang Formation in Yan'an, Ordos Basin; the gas production capacity of Well Liuping 177 reached 2350 m^3/day to become the first continental shale gas well in China [1,2]. After the recent discovery of continental shale gas in the Mesozoic Chang 7 member of Yanchang Formation, Yanchang Petroleum Group breakthroughs have also been made in the Paleozoic era Shanxi Formation in the Yan'an area more than Chang 7 shale gas wells, including Yunyeping 3, Yunyeping 4, Yunyeping 5, and Yunyeping 5-1. Moreover, total daily test production exceeds 6×104 m^3; other gas wells in the Shanxi Formation mud interval show favorable well log analyses and reveal the Ordos Basin's great resource potential and exploration prospects [1,3-9].

Various scholars have conducted studies on the characteristics, pore types, full pore diameter structure characterization, and gas-bearing properties of shale gas reservoirs in the Shanxi Formation [10-16]; the pore types and pore diameter distribution of the shale are thought to be the principal factors affecting adsorption performance. Scholars studying the gas-bearing properties of shale reservoirs believe that the TOC content is an important factor in controlling gas content and bearing capacity

**Corresponding author:* Zhao Weiwei, School of Earth Sciences and Engineering, Xi'an Shiyou University, Xi'an, Shaanxi, China
E-mail addresses: zhaoww@xsyu.edu.cn
Received 2022-04-20, Received in revised form 2023-09-22, Accepted 2024-04-22, Available online 2024-05-02

[16,17]. However, there is a lack of further study on the effects of different genetic pores and their structural characteristics on the adsorption capacity of shale in the Shanxi Formation. Shale gas occurs in shale pores. Thus, studying the types, structural characteristics, and gas-bearing properties of shale pores is essential to understanding shale enrichment mechanisms and direct gas exploration and development. By utilizing argon ion polishing, scanning electron microscopy (SEM), N_2 adsorption, CO_2 adsorption, and the high-pressure methane isothermal adsorption experimental method, well Quan 56, Shan 1, Shanxi Formation of mud shale in Yan 'an area, Ordos Basin was studied.

The pore structure characteristics and oil and gas potential of Shanxi Formation shale were explored, which it provides a geological basis for shale gas exploration and development.

Geological Settings

The Ordos Basin is a typical sedimentary basin rich in oil and gas. Several sets of lacustrine shale, rich in organic matter, were formed during the sedimentary basin's stable subsidence stage. The basic geological conditions favor shale gas enrichment and indicate vast resource potential [8-9]. The mud shale is primarily produced through river delta deposition in the Yan'an area of the Shanxi Formation. The shale accumulated to a thickness of 40–90 m and included a period of Shan 1 member mud shale deposition with a thickness is 20–50 m. Furthermore, the lithology is primarily characterized by a dark gray mud shale film, dark gray tones of sandy shale (or a thin clipped sandstone layer), colored carbonaceous shale (a thin coal seam), and gray, fine-grained sandstone with argillaceous stripes. Shan 2 member of sandstone is more developed and features a larger coal seam than Shan 1 member, composed of dark mudstone, gray-black silty shale, fine sandstone, and an interbedded coal seam [17-18]. The sedimentary facies belt of the Shanxi Formation is characterized by a banded distribution in the N-NE direction [18]. The sedimentary microfacies are more controlled the shale reservoir, and the distribution of the mud shale microfacies is closely related to those of the distributary channel [8,19]. The organic carbon content of the shale in the Shan 1 Member is 0.78%–2.78% (average of 0.598%). The organic carbon content is highly heterogeneous in the vertical distribution, with a Ro value of 2.66%~2.81% (average of 2.66%). The peak temperature (Tmax) is 316–573 °C, with an average of 388.1 °C. The degree of the thermal evolution of the organic matter is in the over-mature stage (Table 1). The mineral composition of the Shan 1 mud shale primarily includes clay minerals and quartz.

Table 1 Statistical table of geochemistry, mineral composition, and pore structure of Shan 1 member shale of Well Quan 56 in the Yan'an area

Sample	Depth(m)	Zone	Lithology	Ro(%)	TOC(%)	Tmax (°C)	Clay Mineral(%)	Quartz(%)	Feldspar(%)	Calcite(%)	Siderite(%)	Specific Surface Area(m^2/g)	Pore Volume (cm^3/g)	Average Pore Diameter(nm)
SQ-1	3059.6	Shanxi Formation	Grey Mudstone	2.53	0.08	424	65	33	2	0	0	4.4124	0.012094	10.9638
SQ-2	3060.2	Shanxi Formation	Grey Mudstone	2.58	0.09	364	64	31	5	0	0	5.0787	0.014324	11.2817
SQ-3	3063.4	Shanxi Formation	Dark gray mudstone interspersed with fine sandstone	2.81	0.12	366	63	37	0	0	0	1.8934	0.009511	20.0928
SQ-4	3067.4	Shanxi Formation	Gray Silty Mudstone	2.59	0.09	372	65	35	0	0	0	6.7565	0.015232	9.0176
SQ-5	3068.8	Shanxi Formation	Gray Silty Mudstone	2.68	0.08	365	55	43	0	0	2	5.6098	0.013383	9.5427
SQ-6	3075.9	Shanxi Formation	Black Mudstone	2.74	0.24	379	25	11	0	0	64	2.6781	0.006607	9.8681
SQ-7	3077.3	Shanxi Formation	Grayish Black Mudstone	2.71	0.14	365	74	26	0	0	0	10.6743	0.018545	6.9494
SQ-8	3079.1	Shanxi Formation	Dark Gray Silty Mudstone	2.57	0.97	316	78	22	0	0	0	6.5078	0.015962	9.8109
SQ-9	3080.6	Shanxi Formation	Dark Gray Silty Mudstone	2.62	0.91	316	67	31	0	0	2	5.4415	0.015415	11.3311
SQ-10	3083.3	Shanxi Formation	Black Silty Mudstone	2.66	1.08	363	66	30	4	0	0	7.3798	0.017243	9.346
SQ-11	3085.4	Shanxi Formation	Gray Siltstone	2.71	0.35	368	64	32	1	0	3	2.2529	0.008012	14.2248
SQ-12	3086.2	Shanxi Formation	Black Mudstone	2.73	2.78	573	55	41	0	2	2	6.8451	0.015215	7.1623
SQ-13	3088.2	Shanxi Formation	Black Mudstone	2.68	0.27	364	71	28	1	0	0	7.5449	0.014224	7.5407
SQ-14	3096.1	Shanxi Formation	Black Silty Mudstone	2.65	1.58	524	60	35	1	0	4	6.2116	0.01693	10.9025
SQ-15	3100.9	Shanxi Formation	Gray fine sandstone interlaced with mudstone strips	2.69	0.19	362	50	42	0	3	5	3.0003	0.008373	11.1629

Results from XRD analysis of 15 samples in this study indicated that clay minerals accounted for 25%–78% of the total compositions (average of 61%). The average contents of quartz, feldspar, calcite, and siderite are 32%, 2%, 3%, and 5%, respectively (Table 1). No pyrite distribution is observed. The macerals of the mud shale kerogen in the Shan 1 member of the Shanxi Formation are mainly vitrinite, inertinite, and exinite, but they do not contain sapropelite. The average content of exinite components (all humic and implantable forms) is 37%, vitrinite is 48%, and inertinite is 15%. Based on the analysis of the type coefficient of organic matter (average -32.7) combined with the pyrolysis parameters of rocks, the type of organic matter in the mud shale of Shan 1 member of Shanxi Formation is type III, and the type of organic matter is humic kerogen; moreover, stratigraphic column of the Shan 1 member of the Quan 56 well location and comprehensive map in the Yan'an area.

Samples and Methods

Mud shale samples were collected from Well Quan 56 in the Yan'an Area of the Shan 1 member of the Shanxi Formation, Ordos Basin. The lithology is primarily black shale (ash), silty mudstone, argillaceous siltstone, or thin layers of fine sandstone. Furthermore, the location and distribution of Well Quan 56 and a single well comprehensive analysis are shown in Fig. 1. Moreover, the lithological characteristics, mineral composition, and organic geochemical parameters of the mud shale samples are shown in Table 1.

Fifteen mud shale samples from the Shan 1 member of the Shanxi Formation of Well Quan 56 in the Yan'an Area were selected for testing and analysis. The thick mudstone samples are selected and sampled in sections. The Engineering Technology Test Center of Sichuan Province tested and analyzed all the mud shale samples. The SEM-EDS samples were polished by a Gatan argon ion-beam etching system at 685 °C. The polished surface of the mud shale was observed with a Zeiss Sigma 300 SEM. An X'Pert multi-functional powder X-ray diffractometer (Panaco Co., Netherlands) was used to analyze the shale vitrinite reflectance for shale mineral composition analysis. An Axio Scope A1 polarizing microscope (Zeiss, Germany) was used with a spectrophotometer to analyze the TOC content. A CS230 carbon-sulfur analyzer (LECO, United States) was also used. Nitrogen adsorption experiments were conducted with a MicroActive ASAP 2460 (United States) to determine the specific surface and pore size automatically. The high methane isothermal adsorption experiment was conducted using an ISOSORP-HP Static II (Rubotherm GmbH, Germany) for high-pressure isothermal adsorption instrument testing.

Results and Discussion

Mud Shale Pore Characteristic of the Shan 1 Member

Most recent studies on the microscopic pore types of mud shale reservoirs in the Ordos basin have focused on the mud shale of the Yanchang Formation. The contact relationship between the mineral composition and the pore types can be divided into three categories: organic pores, mineral pores, and microfractures [20]. However, there are few studies on the pore characteristics of mud shale in the Shanxi Formation [21]. Through a polarizing microscope and scanning electron microscope, the shale pores of the Shanxi Formation can be divided into three categories: organic and mineral pores and microfractures. The mineral pores feature mineral grains or bioclastic particles inside intragranular pores, mineral grains or crystals between pores and intergranular pores, and acid dissolution formed by different dissolution pores.

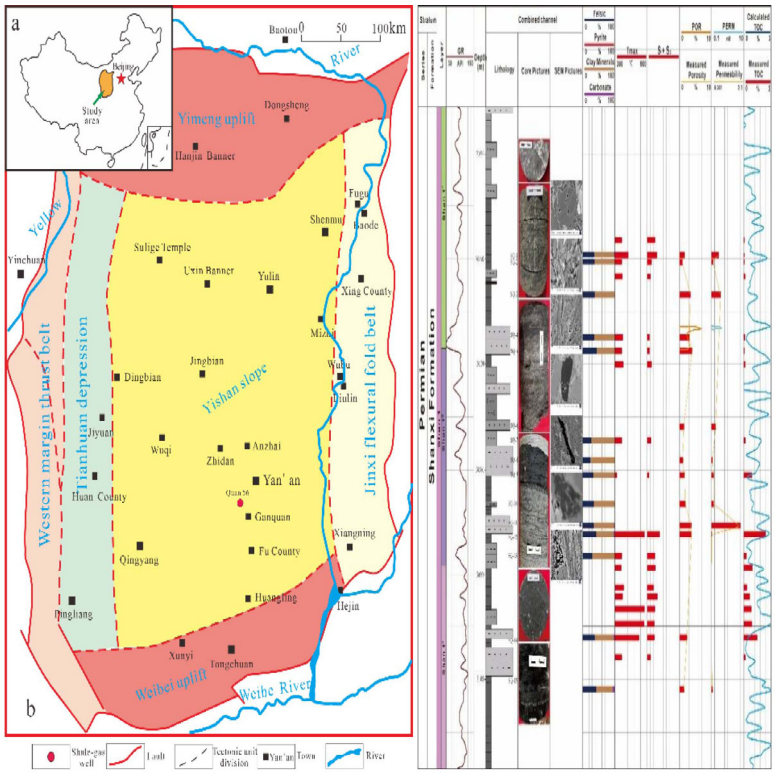

Fig. 1 Stratigraphic column of the Shan 1 member of the Quan 56 well location and comprehensive map in the Yan'an area.

Organic Matter Pore Characteristics

The mud shale samples of Well Quan 56, Shan 1 member of the Yan'an area, were polished with argon ions and observed by SEM. The scattered organic matter of mud shale in Shan 1 member presents a banded directional arrangement (Fig. 2a), and the organic matter pores are relatively less developed (Figs. 2b-f).

The shale belt primarily featured organic shrinkage joint seams (or post holes) and nearly elliptic, conical, polygonal, and irregularly striped pore shapes (Figs. 2g-i). The organic matter pores have diameters between 1.5 nm and 870 nm with an average of approximately 25 nm, and pores with diameters of less than 30 nm predominate.

The types of organic matter in the Shan 1 member shale of the Shanxi Formation are divided into enriched and dispersed states. Enriched organic matter is large, forms isolated blocks with regular shapes, and has an angular or elliptic distribution. The size of the organic matter particles varies from several microns to hundreds of microns, and the contact boundary with inorganic minerals is delineated (Figs. 2b-f). Dispersed organic matter is primarily interwoven with siderite, rutile aggregate, and clay minerals and densely distributed in pores (Figs. 2g–i).

Dispersed organic matter particles are small, banded, and contain clay mineral or rutile aggregate fillings. Organic matter pores are more developed. Dispersed organic matter particles are more affected by the surrounding mineral particles than enriched organic matter and have more complex pore shapes and distributions.

Inorganic Pore Characteristics

The inorganic pores in mud shale of Shan 1 member primarily include mineral intergranular pores, intragranular pores, and dissolution pores (Fig. 3). Compared with marine shale, the content of brittle minerals such as quartz and feldspar in Shan 1 member of the Shanxi Formation of QUAN 56 is relatively small. The content of clay minerals is relatively high (Table 1).

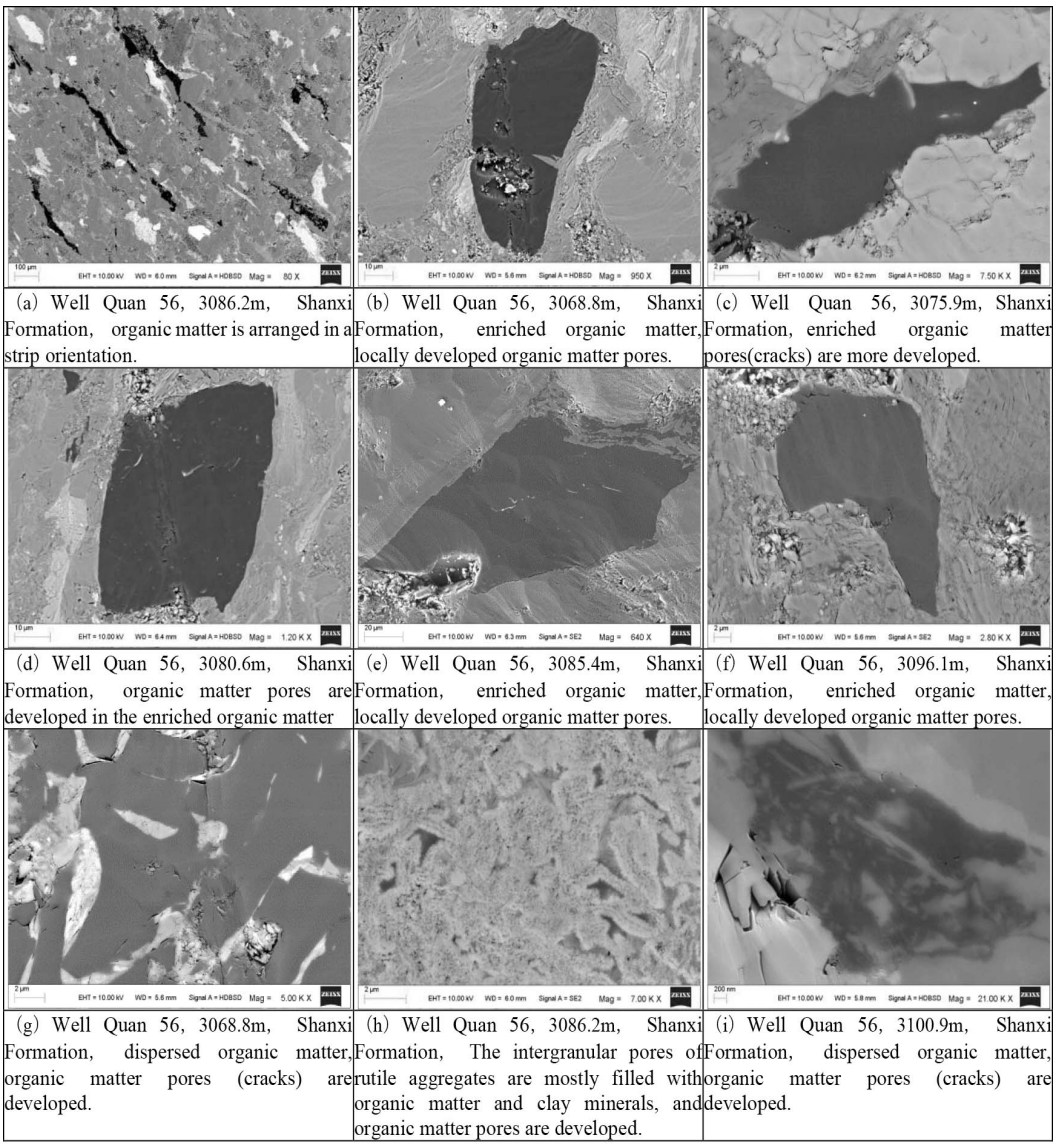

(a) Well Quan 56, 3086.2m, Shanxi Formation, organic matter is arranged in a strip orientation.

(b) Well Quan 56, 3068.8m, Shanxi Formation, enriched organic matter, locally developed organic matter pores.

(c) Well Quan 56, 3075.9m, Shanxi Formation, enriched organic matter pores(cracks) are more developed.

(d) Well Quan 56, 3080.6m, Shanxi Formation, organic matter pores are developed in the enriched organic matter

(e) Well Quan 56, 3085.4m, Shanxi Formation, enriched organic matter, locally developed organic matter pores.

(f) Well Quan 56, 3096.1m, Shanxi Formation, enriched organic matter, locally developed organic matter pores.

(g) Well Quan 56, 3068.8m, Shanxi Formation, dispersed organic matter, organic matter pores (cracks) are developed.

(h) Well Quan 56, 3086.2m, Shanxi Formation, The intergranular pores of rutile aggregates are mostly filled with organic matter and clay minerals, and organic matter pores are developed.

(i) Well Quan 56, 3100.9m, Shanxi Formation, dispersed organic matter, organic matter pores (cracks) are developed.

Fig. 2 Organic matter pore characteristics of shale in Shan 1 member of Well Quan 56 in the Yan'an area.

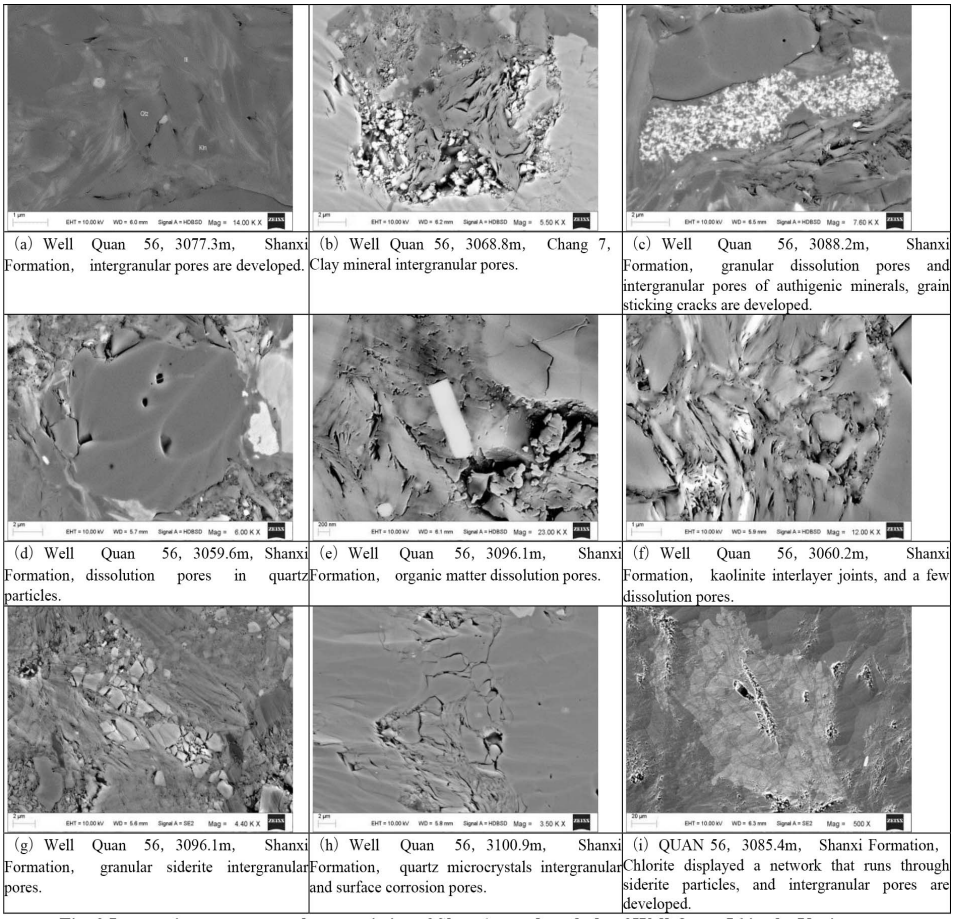

(a) Well Quan 56, 3077.3m, Shanxi Formation, intergranular pores are developed.

(b) Well Quan 56, 3068.8m, Chang 7, Clay mineral intergranular pores.

(c) Well Quan 56, 3088.2m, Shanxi Formation, granular dissolution pores and intergranular pores of authigenic minerals, grain sticking cracks are developed.

(d) Well Quan 56, 3059.6m, Shanxi Formation, dissolution pores in quartz particles.

(e) Well Quan 56, 3096.1m, Shanxi Formation, organic matter dissolution pores.

(f) Well Quan 56, 3060.2m, Shanxi Formation, kaolinite interlayer joints, and a few dissolution pores.

(g) Well Quan 56, 3096.1m, Shanxi Formation, granular siderite intergranular pores.

(h) Well Quan 56, 3100.9m, Shanxi Formation, quartz microcrystals intergranular and surface corrosion pores.

(i) QUAN 56, 3085.4m, Shanxi Formation, Chlorite displayed a network that runs through siderite particles, and intergranular pores are developed.

Fig. 3 Inorganic matter pore characteristics of Shan 1 member shale of Well Quan 56 in the Yan'an area.

The intergranular pores in the shale are not only intergranular pores between clay minerals but also quartz, feldspar, rigid particles, and clay minerals. Minerals are often scattered with rigid particles or embedded in clay and organic matter and do not easily form particles. Intergranular pore development is low, primarily manifested through slight brittleness between mineral grains or particles and clay minerals. Pores are nearly round or polygonal with apertures of tens of nanometers. Intergranular siderite pores in the Shan 1 member are widely developed. Siderite masses are often strongly dissolved and partially filled with and surrounded by organic matter. When the content of rigid clastic particles such as feldspar and quartz is relatively high in the thin layer of fine sandstone or silty laminae, during the compaction process, the rigid clastic particles such as quartz and feldspar contact and support each other, and the primary intergranular pores can be formed (Fig. 3a). The pore shape is an irregular polygon. Most pore diameters are between ten nanometers and a few microns. At the same time, the shielding effect of rigid particles makes the compacting of intergranular interpores between rigid particles relatively weak, and there are more intergranular pores between rigid particles, fine intergranular interpores, and intersedimentary interpores (Fig. 3b,c). These intergranular pores are mostly linear, polygonal, or elliptic in shape, with pore sizes ranging from 5 nm to 100 nm and up to 2 μm. Some unstable minerals, such as feldspar particles and carbonate cement, were dissolved at the edge of the particles under the action of an acidic solution, presenting harbor dissolution pores and forming intergranular dissolution expansion pores (Fig. 3 d,e) with pore sizes ranging from 100 nm. Some of the primary intergranular pores or intergranular dissolution expansion pores are filled by authigenic quartz, authigenic clay minerals, and other cement and complexes, leading to smaller intergranular pores and the formation of residual intergranular pores. Late fluids also dissolve some cement-filled dissolution expansion pores or larger primary intergranular pores to form intergranular and intragranular dissolution pores. In the diagenetic process of mud shale, there are many intercrystalline pores in the authigenic minerals such as authigenic quartz, feldspar cement, and carbonate cement between clastic particles or in the dissolution pores (Fig. 3d), and some crystal edges are also dissolved. The inter-crystal pores are of various forms, mainly narrow, long, linear, and irregular polygonal pores. The size of inter-crystal pores varies from 7 nm to 300 nm. A few residual intergranular pores are also developed between authigenic minerals and clastic particles (Fig. 3c).

Intra-grain pores (pores developed inside grains) are primarily formed by mineral dissolution, including intergranular pores inside clay minerals and siderite particles. The coexistence of organic matter and inorganic minerals in shale during the evolution of organic matter hydrocarbon generation releases abundant organic acids and CO_2. The dissolution of quartz, feldspar, carbonate, and other soluble minerals of the edges and interiors of mineral grains by organic acids produces multiple dissolution pores. Microscopic observations revealed dissolution pores widely distributed on intragranular pore surfaces in quartz, feldspar, dolomite, and clay minerals (Figs. 3c–f). Furthermore, pore sizes ranged from tens of nanometers to several microns, and pore shapes included long axial joints, ellipses, circles, and irregular polygons (Figs. 3g-3h).

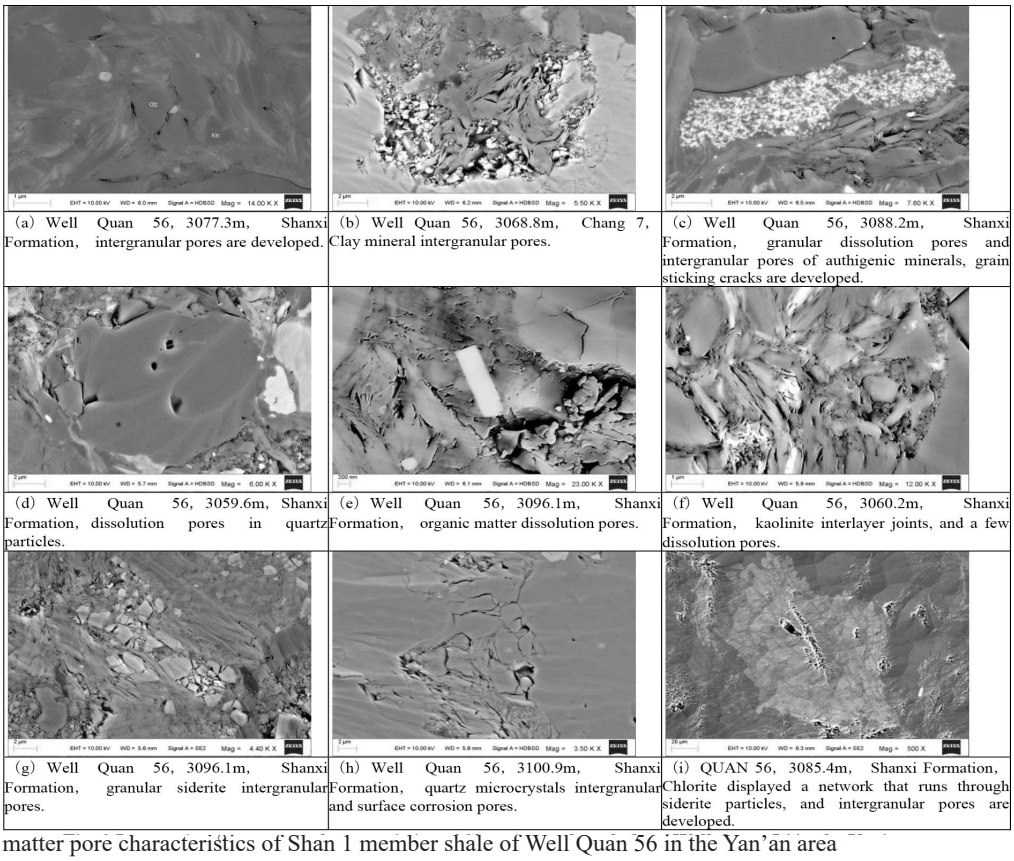

(a) Well Quan 56, 3077.3m, Shanxi Formation, intergranular pores are developed.
(b) Well Quan 56, 3068.8m, Chang 7, Clay mineral intergranular pores.
(c) Well Quan 56, 3088.2m, Shanxi Formation, granular dissolution pores and intergranular pores of authigenic minerals, grain sticking cracks are developed.
(d) Well Quan 56, 3059.6m, Shanxi Formation, dissolution pores in quartz particles.
(e) Well Quan 56, 3096.1m, Shanxi Formation, organic matter dissolution pores.
(f) Well Quan 56, 3060.2m, Shanxi Formation, kaolinite interlayer joints, and a few dissolution pores.
(g) Well Quan 56, 3096.1m, Shanxi Formation, granular siderite intergranular pores.
(h) Well Quan 56, 3100.9m, Shanxi Formation, quartz microcrystals intergranular and surface corrosion pores.
(i) QUAN 56, 3085.4m, Shanxi Formation, Chlorite displayed a network that runs through siderite particles, and intergranular pores are developed.

Fig. 3 Inorganic matter pore characteristics of Shan 1 member shale of Well Quan 56 in the Yan'an area

The vitreous reflectance of the mud shale in the Shanxi Formation averaged 2.66%; the entire shale layer was in the dry gas generation stage. The organic matter of the mud shale formed multiple organic acids with hydrocarbon generation and easily dissolved various minerals. Moreover, the montmorillonite in the mud shale in the Shan 1 Member produced numerous intracellular pores during conversion to Yi/montmorillonite or illite. Furthermore, clay minerals with poor chemical stability are easily converted into Yi/montmorillonite through diagenesis, forming numerous interlaminar pores (Fig. 3i) during the transformation process. In addition, pore connectivity is excellent and provides important storage space and migration channels for continental shale gas. The dissolution pores in the quartz grains are relatively well-developed in the mud shale, with pore diameters of approximately 10–100 nm. The dissolution pores generally feature poor connectivity but facilitate the enrichment and storage of shale gas. A few mold holes were observed, including sol junctions between mold particles.

Microfracture Characteristics

Microfracture is an important pore space type in the Shan 1 member shale reservoir [22]. Microscopic thin sections and SEM reveal that the layered clay rock section lines of Well Quan 56, Shan 1 member, Shanxi Formation developed micro-cracks in the argillaceous siltstone (Fig. 4). The primary types of microfracture are flaky schistosity between clay minerals (Fig. 4b), mineral particle (Fig. 4b), organic matter internal shrinkage joints (Fig. 4c), organic matter (Figs. 4d, 4e) between particles and between clay mineral seam layers (Figs. 4f–h), and particle internal microfracture (Fig. 4i). The organic matter contraction joints (adherent joints) are primarily microfractures formed between debris particles and flaky clay minerals, with widths ranging from 30 to 600 nm. Microfractures develop within the organic matter or between particles of organic matter, with widths between 20 and 150 nm. Interlaminar fractures formed by clay mineral layers primarily develop in the interlamellar layers, where clay minerals interact with organic matter. The length of the interlaminar fractures is related to the length of the clay mineral.

Mud Shale Pore Structure Characteristics

Mud Shale Nitrogen Adsorption Curve

Cryogenic nitrogen adsorption and desorption experiments were conducted on 15 mud shale samples in Well Quan 56 of the Shan 1 member. Also, the analyzed specific pore surface area, pore volume, average pore diameter, and nitrogen (N_2) adsorption test results are shown in Table 1. The mud shale types of the Shan 1 member had a type IV adsorption curve according to the International Federation of Pure and Applied Chemistry (IUPAC) classification. The nitrogen adsorption quantity gradually increases as relative pressure increases, producing a reverse "S-type" curve (Fig. 5). The mud shale of the Shan 1 member pore is in an open state with relatively high pressure. The desorption isotherm is located in the upper part of the adsorption isotherm and forms a hysteresis loop. The hysteresis shape partially reflects the porosity of the porous media and represents mesoporous and macroporous capillary condensation. According to the IUPAC classification, the hysteresis of the Well Quan 56 mud shale samples are of the H3 type and reflect a relatively complex pore structure and the development of various irregular micropores and mesopores. The ink bottle-shaped neck of the well is open on both ends. The parallel slit pores in the tube hole wall are intergranular, and a horizontal bedding layer seam separates the strongly heterogeneous pore types.

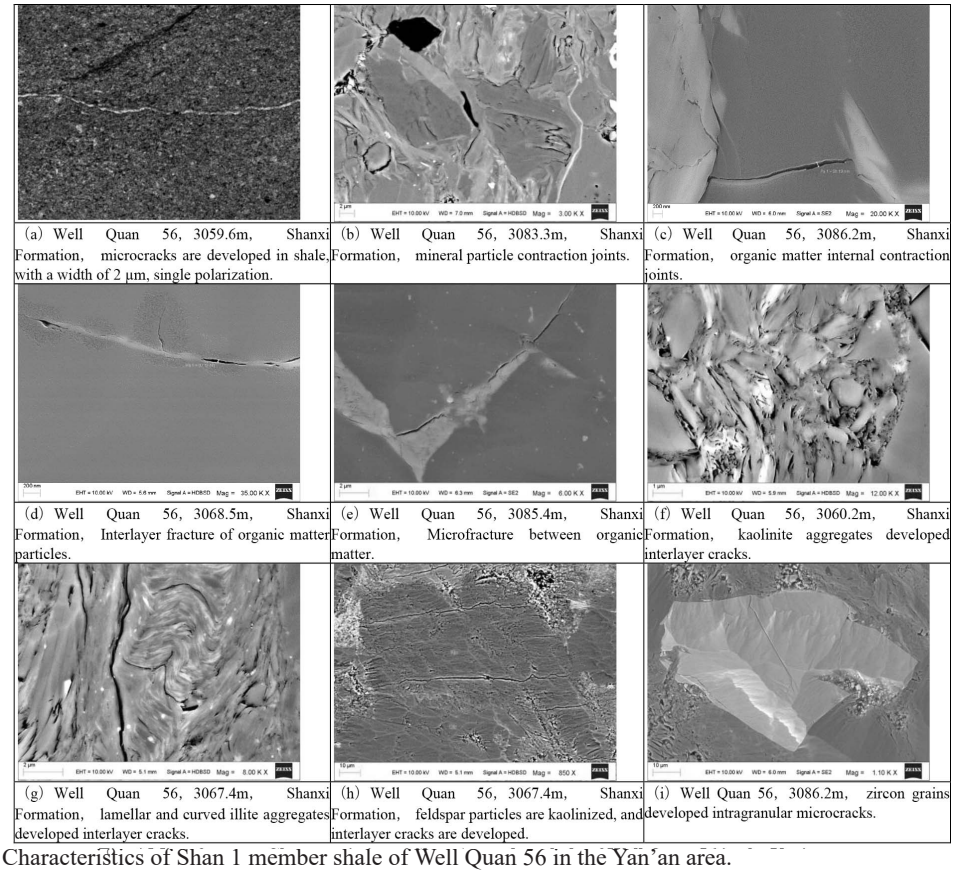

(a) Well Quan 56, 3059.6m, Shanxi Formation, microcracks are developed in shale, with a width of 2 μm, single polarization.

(b) Well Quan 56, 3083.3m, Shanxi Formation, mineral particle contraction joints.

(c) Well Quan 56, 3086.2m, Shanxi Formation, organic matter internal contraction joints.

(d) Well Quan 56, 3068.5m, Shanxi Formation, Interlayer fracture of organic matter particles.

(e) Well Quan 56, 3085.4m, Shanxi Formation, Microfracture between organic matter.

(f) Well Quan 56, 3060.2m, Shanxi Formation, kaolinite aggregates developed interlayer cracks.

(g) Well Quan 56, 3067.4m, Shanxi Formation, lamellar and curved illite aggregates developed interlayer cracks.

(h) Well Quan 56, 3067.4m, Shanxi Formation, feldspar particles are kaolinized, and interlayer cracks are developed.

(i) Well Quan 56, 3086.2m, zircon grains developed intragranular microcracks.

Fig. 4 Microfracture Characteristics of Shan 1 member shale of Well Quan 56 in the Yan'an area.

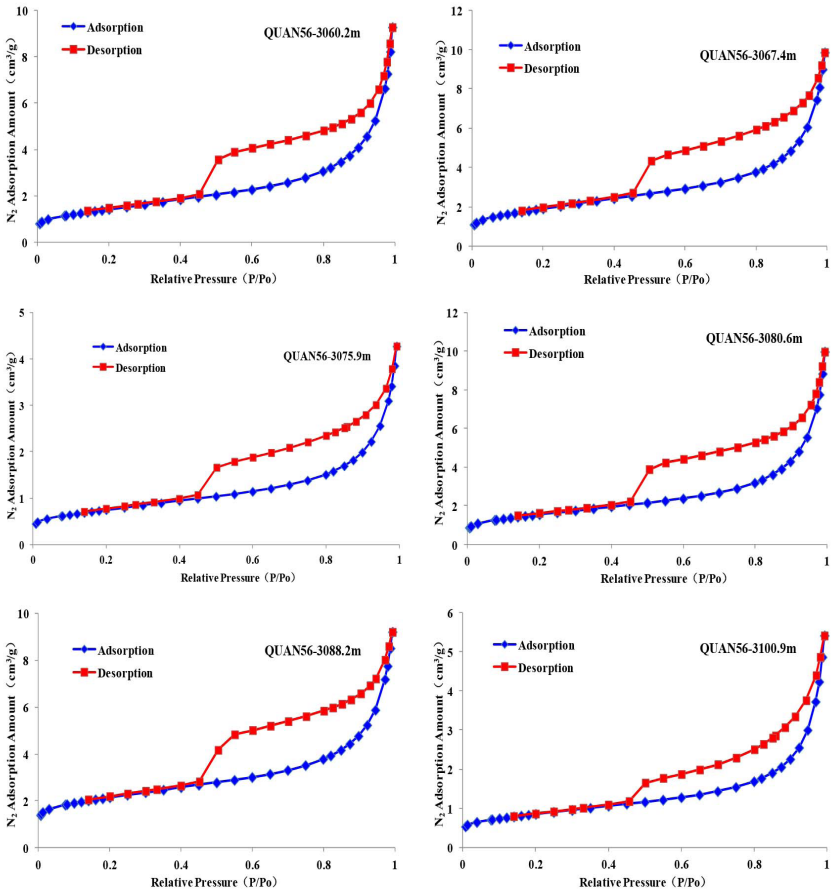

Fig. 5 Characteristics of cryogenic nitrogen adsorption/desorption isothermal curves of Shan 1 member shale of Well Quan 56 in Yan'an area

Additionally, the hysteresis loop forms a "forced closure" phenomenon ranging from P/Po = 0.4~0.5. Groen and others proposed that forced closure is related to the tension strength effect that is believed to be caused by strong instability of the hemispherical bending liquid level in pores smaller than 4 nm during desorption. Thus, the shale samples contain numerous pores smaller than 4 nm [23].

Specific Surface Area and Pore Volume of the Mud Shale

The specific surface area and pore volume of shale are indexes reflecting the adsorption capacity and pore quantity, respectively. The pore-specific surface area of Shan 1 Member mud shale of Well Quan 56, Yan'an area ranges from 1.8934~10.6743 m^2/g (average of 5.4858 m^2/g). The average shale pore size distribution ranges from 6.9494–20.0928 nm; the pore volume distribution of the mud shale ranges from 6.6×10-3~18.545×10-3 cm^3/g (average of 13.4×10-3 cm3/g and) and shows strong heterogeneity (Fig. 6). The specific pore surface area and the pore volume are generally positively correlated with the N2 adsorption (Figs. 7 and 8). Therefore, larger specific pore surface areas and pore volumes yield greater gas adsorption and a greater proportion of micropores in mud shale.

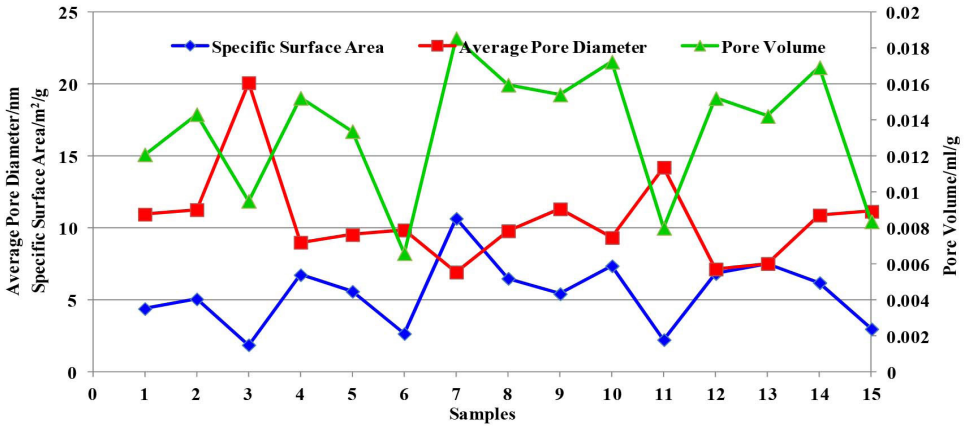

Fig. 6 Pore structure parameter of Shan 1 member shale samples of Well Quan 56 in the Yan'an area.

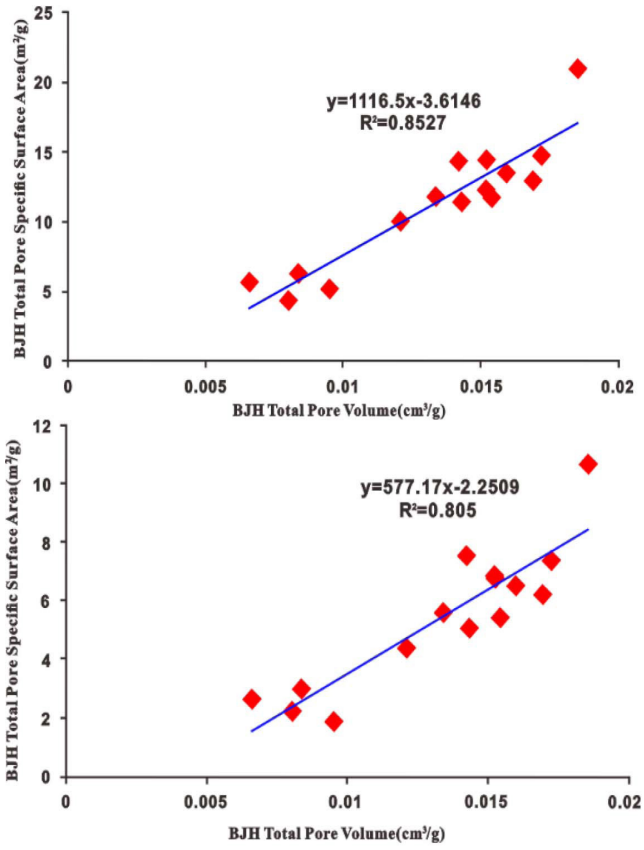

Fig. 7 Diagram of total pore specific surface area and total pore volume of Shan 1 member shale of Well Quan 56 in Yan'an area.

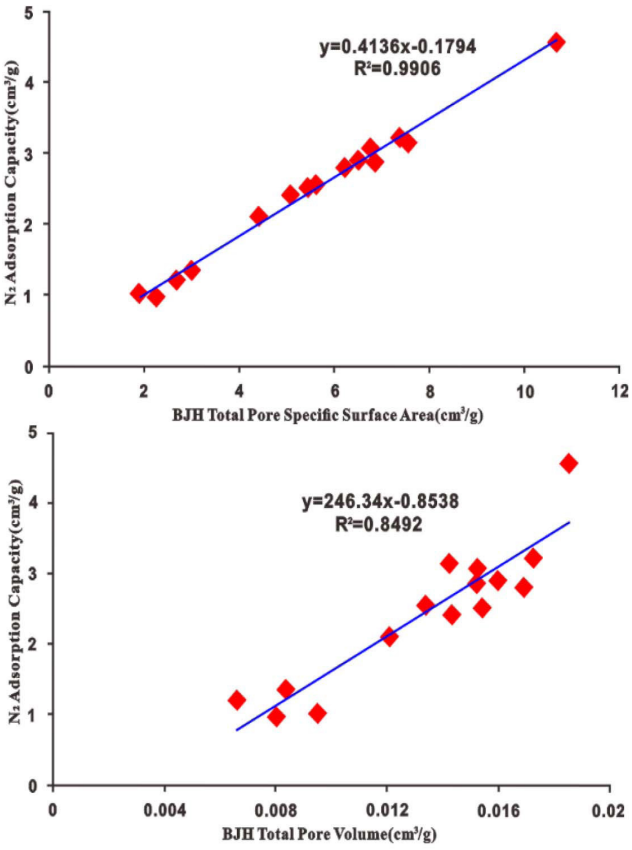

Fig. 8 The relationship between total pore specific surface area, total pore volume, and N2 adsorption capacity of Shan 1 member mud shale of Well Quan 56 in Yan'an area.

Analysis of the N_2 adsorption experiment reveals that the pore diameters of the Shan 1 member mud shale of Well Quan 56, Shanxi Formation, range from 1.8~254 nm and are primarily mesopores with sizes of 3~5 nm. Pore sizes between 3 nm and 5 nm account for greater pore volume and specific surface area than pore sizes larger than 5 nm (Fig. 9). Most of the pores in the 3~5 nm range are primarily organic matter hydrocarbon holes, clastic particle dissolution pores, and pores between clay mineral crystals.

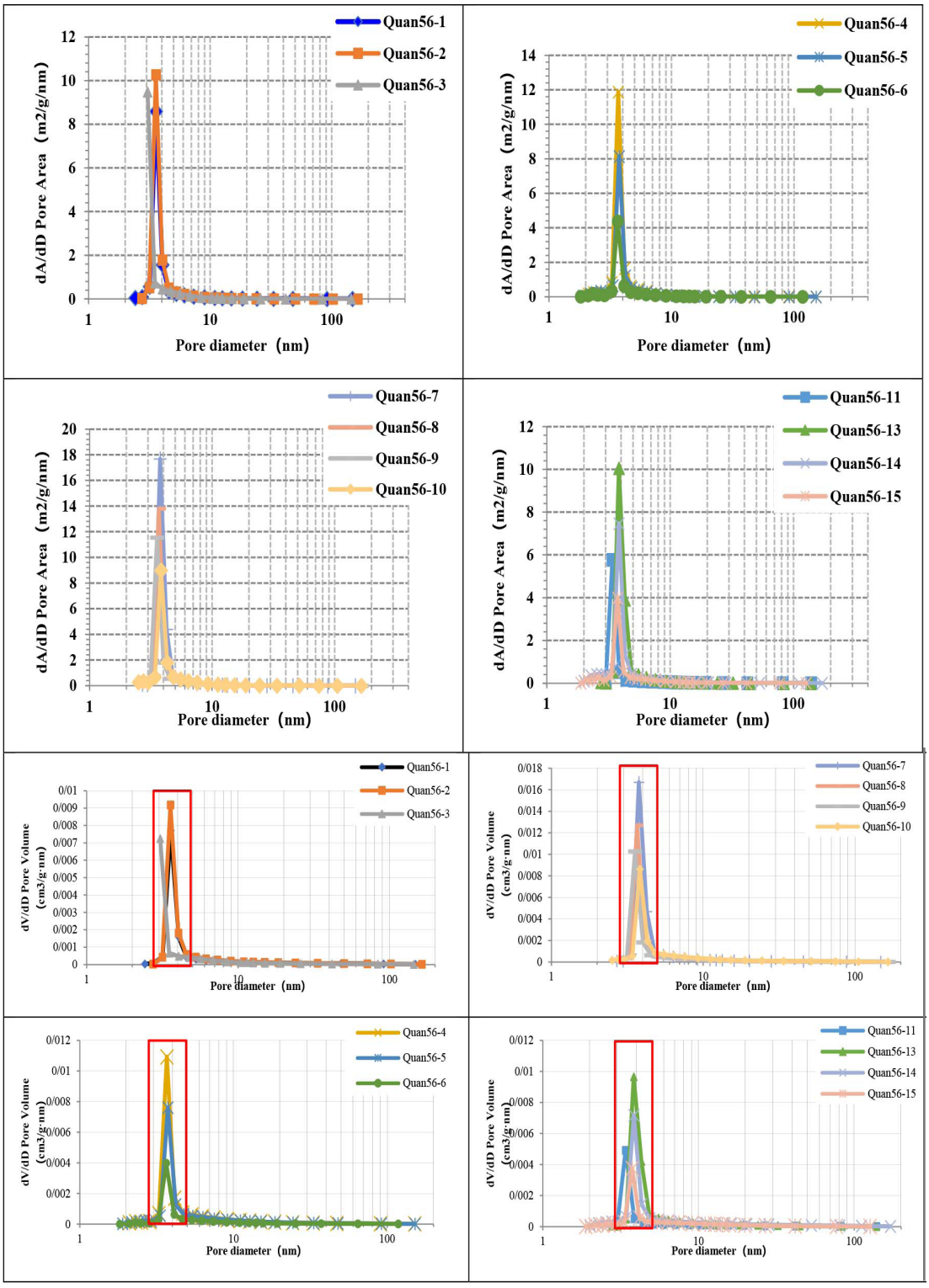

Fig. 9 Diagram of the relationship between BJH average pore diameter of Shan 1 member mud shale and pore volume in BJH stage.

CO_2 Adsorption

The distribution characteristics and the proportion of shale micropores are further analyzed with a CO_2 adsorption experiment. The sizes of the mudstone micropores in Well Quan 56, Shan 1 member, Yan'an area range from 0.5~0.6 nm and 0.8~0.9 nm.

The pore-specific surface area and pore volume change rate for pore sizes between 0.5 nm and 0.6 nm account for the greatest pore volume and specific surface area (Fig. 10). The CO_2 adsorption experiment shows that pore diameters of 0.5~0.6 nm accounted for the largest pore volume and specific surface area in the Shan 1 member shale. Therefore, the intergranular pores of clay minerals account for the largest specific surface area and volume in the micropores. Higher clay mineral contents coincide with greater pore volume and specific surface area contributions.

Pore Size Distribution

The aperture size distribution characteristics of the Shan 1 member shales in Well Quan 56 are further characterized. Experimental methods for determining the pore size precision and range of the shale include high-pressure mercury injection (from 50 nm to 20 m), N_2 adsorption (2–50 nm), and CO_2 adsorption (<2 nm) to determine the pore volume and specific surface area and to characterize the general pore size distribution of the shale in the study area.

The pore volume and total pore size statistics of the Shan 1 member mud shale (Table 2) reveal the development of different pore sizes in Well Quan 56. Mesopores and micropores are dominant (except in Quan 56-10, Quan 56-11, and Quan 56-15), and the pore size distribution is heterogeneous. The average pore volume of the mud shale in Well Quan 56, Shan 1 member, is 0.0014 ml/g and accounts for 13.41% of the total pore volume. Medium pore volume accounted for the highest proportion of total pore volume (0.01046 ml/g, 66.24%). The average pore volume is 0.0075 ml/g, accounting for 25.34% of the total pore volume. Therefore, the pore volume distribution in the mud shale in the study area is dominated by mesopores, followed by macropores and micropores.

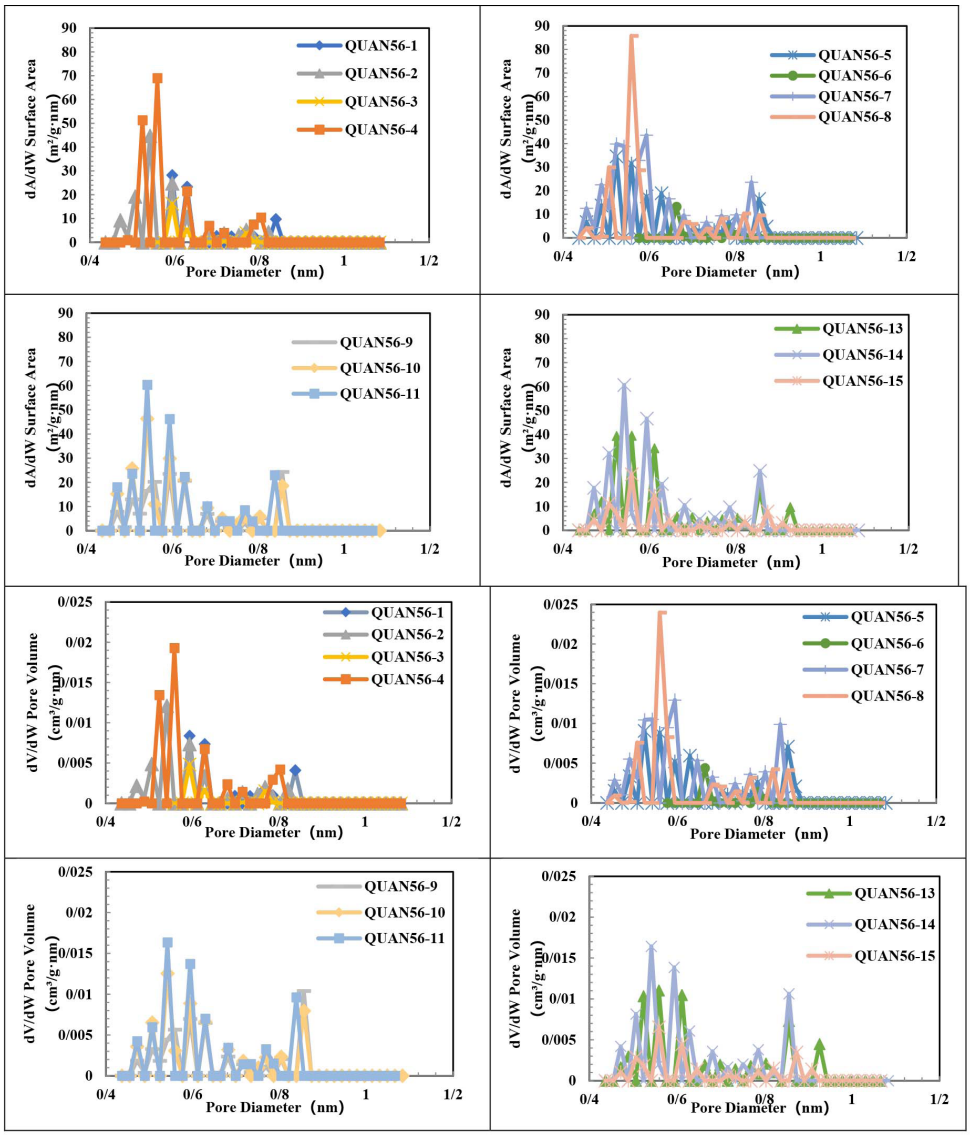

Fig. 10 Pore volume and specific surface area change rates calculated by CO_2 adsorption experiments of Shan 1 member shale of well Quan 56 in the Yan'an area.

Table 2 Statistics of shale volume and pore size distribution in Shan 1 member of well Quan 56 in the Yan'an area.

Sample Number	Pore Volume(ml/g)				Proportion to total volume(%)		
	Micropore	Mesopore	Macropore	Total volume	Micropore	Mesopore	Macropore
QUAN56-1	0.001015	0.009766	0.0008090	0.01159	10.3932	84.2623	6.980155
QUAN56-2	0.001366	0.011639	0.0001551	0.01316	11.7364	88.44158	1.178562
QUAN56-3	0.000637	0.008502	0.002954	0.012093	7.492355	70.30514	24.42735
QUAN56-4	0.001660	0.011672	0.005501	0.018833	14.22207	61.97632	29.20937
QUAN56-5	0.001533	0.010416	0.001342	0.013291	14.71774	78.36882	10.09706
QUAN56-6	0.000526	0.005219	0.0005058	0.006251	10.07856	83.49331	8.091764
QUAN56-7	0.002332	0.013026	0.001078	0.015358	17.90266	79.25286	6.558773
QUAN56-8	0.001850	0.012537	0.003424	0.017811	14.75632	70.38909	19.22408
QUAN56-9	0.001297	0.012544	0.0001057	0.013947	10.3396	89.94242	0.757885
QUAN56-10	0.001787	0.013410	0.01737	0.032567	13.32588	41.17665	53.3362
QUAN56-11	0.001625	0.006870	0.04004	0.048535	23.65357	14.15473	82.49717
QUAN56-13	0.001283	0.010400	0.003249	0.014932	12.33654	69.64908	21.75864
QUAN56-14	0.001957	0.013685	0.002383	0.018025	14.30033	75.92233	13.22053
QUAN56-15	0.000853	0.006813	0.02633	0.033996	12.52018	20.04059	77.45029
Average value	0.001408643	0.010464214	0.007517614	0.0193135	13.41252893	66.24108714	25.34198779

Note: Due to sample Quan56-12, N_2 and CO_2 adsorption experiments were not carried out, and the data were not counted.

The specific surface area of the mud shale in Well Quan 56, Shan 1 member (Table 3) is primarily dominated by mesopores and micropores; macropores generate the less specific surface area. The average specific surface area of micropores in the mud shale of Well Quan 56, Shan 1 member (5.28 m^2/g) accounts for 48.86% of the total. The ratio of mesoporous specific surface area to the total specific surface area averages 5.39 m^2/g, accounting for 49.64% of the total. The average specific surface area of macropores (0.137 m^2/g) accounts for 1.496% of the total. Thus, micropores and mesopores contribute the most to the total specific surface area; macropores contribute the least and are ignored [24,25].

Methane Adsorption Characteristics

A methane isothermal adsorption experiment was conducted to verify the adsorption capacity of the mud shale. Table 4 shows the isothermal adsorption experiment results of methane from mud shale in Shan 1 member, Shanxi formation: At 90 °C, the LAN volume of methane adsorption from mud shale is 9.02~13.02 m^3/t (average of 10.824 m^3/t). The adsorption performances of different shale samples in Shan 1 member differed significantly, primarily due to influencing factors such as the pore type and size distribution.

Table 3 Statistics of shale pore surface area in Shan 1 member of well Quan 56 in Yan'an area.

Sample Number	Specific surface area(m^2/g)				Proportion to total specific surface area(%)		
	Micropore	Mesopore	Macropore	Total specific surface area	Micropore	Mesopore	Macropore
QUAN56-1	3.7577	4.4124	0.002788	8.172888	45.97762749	53.98826	0.034113
QUAN56-2	4.2813	5.0787	0.0004486	9.3604486	45.73819251	54.25701	0.004793
QUAN56-3	1.3904	1.8934	0.04775	3.33155	41.73432787	56.83241	1.433267
QUAN56-4	5.0130	6.7565	0.2219	11.9914	41.80496022	56.34455	1.850493
QUAN56-5	5.2480	5.6098	0.000722	10.858522	48.33070283	51.66265	0.006649
QUAN56-6	10.8409	2.6781	0.06798	13.58698	79.78888612	19.71078	0.500332
QUAN56-7	7.5819	10.6743	0.15263	18.40883	41.18621336	57.98467	0.829113
QUAN56-8	5.7271	6.5078	0.1169	12.3518	46.36652148	52.68706	0.946421
QUAN56-9	4.5839	5.4415	0.004718	10.030118	45.70135665	54.25161	0.047038
QUAN56-10	6.4206	7.3798	0.05097	13.85137	46.35353759	53.27848	0.367978
QUAN56-11	5.3527	2.2529	0.09918	7.70478	69.47245736	29.24029	1.287253
QUAN56-13	3.89892	7.5449	0.279	11.72282	33.25923285	64.36079	2.379973
QUAN56-14	6.4181	6.2116	0.1478	12.7775	50.22970065	48.61358	1.156721
QUAN56-15	3.4509	3.0003	0.7248	7.176	48.08946488	41.8102	10.10033
Average value	5.283244286	5.388714286	0.136970471	10.80892904	48.85951299	49.64445289	1.496034119

Note: Due to sample Quan56-12, N2 and CO_2 adsorption experiments were not carried out, and the data were not counted.

Table 4 Statistical table of methane adsorption of Shan 1 member mud shale samples in the Yan'an area.

Well	Depth /m	Zone	Lithology	Langmuir's Pressure(MPa)	Langmuir's Volume(m^3/t)
Quan56-1	3059.6	Shanxi Formation	gray mudstone	1.18	11.71
Quan56-2	3060.2	Shanxi Formation	gray mudstone	0.88	11.27
Quan56-3	3063.4	Shanxi Formation	dark gray mudstone interca-lated with fine sandstone	0.61	13.02
Quan56-4	3067.4	Shanxi Formation	gray silty mudstone	0.7	10.25
Quan56-5	3068.8	Shanxi Formation	gray silty mudstone	1.42	9.23
Quan56-6	3075.9	Shanxi Formation	black mudstone	0.84	11.96
Quan56-7	3077.3	Shanxi Formation	gray black mudstone	0.94	11.25
Quan56-8	3079.1	Shanxi Formation	dark gray silty mudstone	1	10.72
Quan56-9	3080.6	Shanxi Formation	dark gray silty mudstone	1.65	9.02
Quan56-10	3083.3	Shanxi Formation	black silty mudstone	1.84	9.91
Quan56-11	3085.4	Shanxi Formation	gray siltstone	1.45	9.76
Quan56-12	3086.2	Shanxi Formation	black mudstone	0.53	12.43
Quan56-13	3088.2	Shanxi Formation	black mudstone	1.16	10
Quan56-14	3096.1	Shanxi Formation	black silty mudstone	1.74	10.03
Quan56-15	3100.9	Shanxi Formation	gray fine sandstone interca-lated with mudstone strip	0.86	11.8

Influencing Factors of Shale Gas Content

Organic Pores

Under the same experimental conditions, the methane adsorption quantity changes much more in the Shanxi Group 1 mud shale. Additionally, the organic carbon content increased (Fig. 11a). Organic matter pores became more numerous as the organic carbon content in the mudstone page increased during the highly mature stage. Consequently, the specific surface area of methane adsorption increased, increasing shale gas adsorption. These results are consistent with those of previous studies [24,25]. Methane adsorption experiments show that the pore diameter distribution characteristics of the Shan 1 member shale were primarily mesoporous and micropores less than 10 nm in size (Fig. 9). The larger specific surface area of the micropores provides more adsorption points for methane molecules and produces stronger gas adsorption capacity. Further, SEM observations reveal that the organic matter pores in the Shan 1 member shale also provided important storage space for gas (Figs. 2 and 3). The rich organic matter content of the reservoir and symbiosis with the clay mineral content of organic matter in mud shale pores increase the organic matter content and the pore-specific surface area and improve the adsorption ability of the shale.

The organic carbon content of the Shan 1 member shale is relatively low (average of 0.598%). The organic carbon mass fraction of the Shan 1 member shale is weakly positively correlated with methane adsorption (Fig. 11a), indicating that the increased organic carbon mass fraction did not significantly increase the number of organic nanopores. However, the high degree of the thermal evolution of Well Quan 56, Shan 1 member shale (Ro average of 2.66%) produces a positive correlation between the organic matter in the raw dry gas phase and methane adsorption quantity and vitrinite reflectance (Fig. 11). However, the low organic matter content is unable to form numerous organic matter pores. The low nitrogen adsorption also leads to a weak negative correlation between pore-specific surface area and the maximum adsorption of methane gas in the shale (Fig. 11).

Inorganic Pores

Inorganic pores are largely primary intergranular pores, clay mineral intergranular pores, dissolution pores, and microfractures in mineral grains. The relative content of the inorganic mineral composition affects the adsorption capacity of shale. The adsorption capacity of the Shan 1 member shale is not controlled by organic matter pores but had a high methane adsorption capacity (Table 4). Thus, the methane adsorption capacity of mudstone shale is affected by the type and content of clay minerals, which are relatively abundant in the Shan 1 member (Table 1). Moreover, abundant inorganic clay minerals (e.g., illite, and montmorillonite) have pore diameters of 1~2 nm and 3~5 nm. The specific surface area and average pore diameter of the Shan 1 member shale are negatively correlated (Fig. 12); therefore, higher clay mineral content and pore hole development lead to smaller average pore radii and specific surface area. The mudstone shale content in Shan 1 member is negatively correlated with the adsorption capacity of the mud shale (Fig. 12b) but positively correlated with the clay mineral content (50%~80%). Therefore, the pores developed by clay minerals account for significant gas adsorption. The experimental results show that the Shan 1 member shale of the Shanxi Formation had a relatively high methane adsorption capacity (Table 4). Dominant clay mineral pores developed in Shan 1 member shale of the Shanxi Formation (Figure 3) also contain micropores that increase the specific surface area of the shale. The content of the Shan 1 member shale has similar methane adsorption and gas content characteristics (Figure 12c). Therefore, increased quartz content in shale reduces the clay mineral content, reducing methane adsorption by clay minerals.

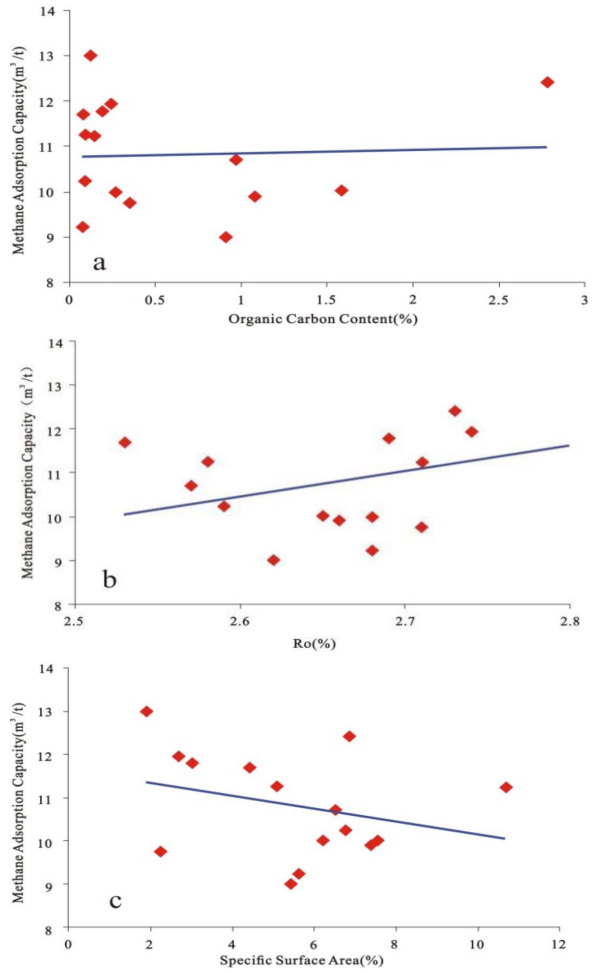

Fig. 11 Chart showing the relationship between methane adsorption and specific surface area, organic carbon content, and Ro in shale well Quan 56, Yan'an area, Shanxi Formation.

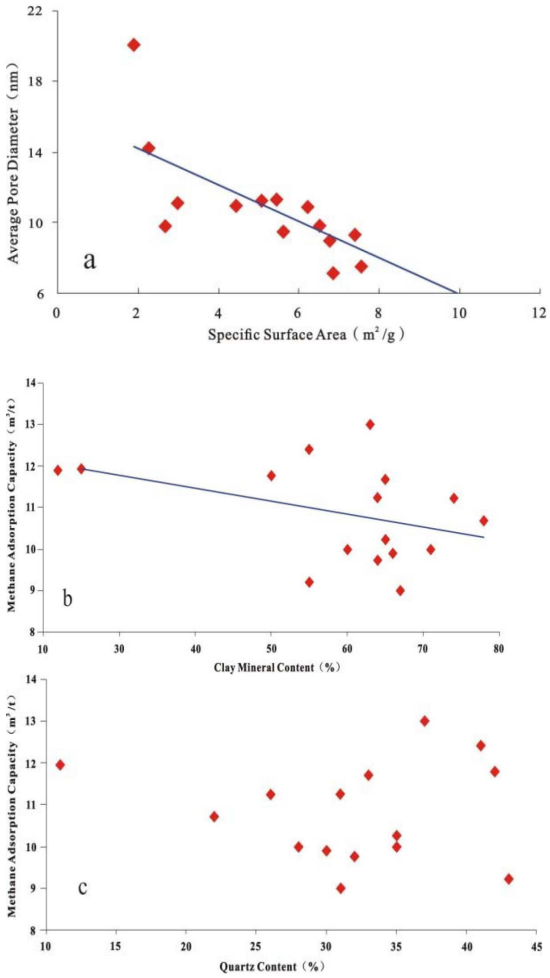

Fig. 12 Relationship between adsorption gas content and minerals content in Shan 1 member shale of well Quan 56 in the Yan'an area

Thermal Maturity

The clay mineral content in the mud shale in the study area is relatively high. Numerous clay mineral pores gradually form as the degree of thermal evolution increases. It further increases the volume and specific surface area of the micropores of the mud shale, thus increasing the gas storage space and adsorption capacity. The low organic carbon content of the shale in the Shan 1 member of the Shanxi Formation affects the adsorption ability of shale. It produces a weak positive correlation with the specific surface area (Fig. 13a) (Ro) and a weak negative correlation with the overall capacity of the shale (Fig. 13b). The correlation between the vitrinite reflectance and specific surface area in the highly mature stage of shale development is not significant. The weak positive correlation between Ro and the organic carbon content (Fig. 13c) indicates that the adsorption capacity of shale increases as the organic carbon content increases. Additionally, the adsorption capacity increases with maturity. Therefore, increasing the maturity of mud shale improves the methane adsorption capacity.

Conclusions

(1) The Shan 1 shale of the Shanxi Formation of well Quan 56 in the Yan'an area has an average thickness of 20~45 m, low organic matter content (TOC average of 0.598%), and highly mature thermal evolution (Ro average of 2.66%). Type III organic matter is dominant. The clay shale primarily comprises clay minerals (25%~78%, average of 61.0%) and quartz (average of 32.0%).

(2) The pore types of mud shale in Shan 1 Member of Shanxi Formation are primarily intergranular and chip pores of clay minerals, followed by microfractures, dissolution pores, and organic matter pores. Different pore types provide effective storage space for shale gas, and the pore size distribution is highly heterogeneous. The pore volume distribution is dominated by mesopores, followed by macropores and micropores, which account for the shale's largest total specific surface area; macropores contribute the least specific surface area.

(3) The gas-bearing properties of the Shan 1 member shales are affected by organic carbon content, mineral composition, and maturity. Higher organic carbon content yields more organic matter pore development, and larger surfaces yield greater methane adsorption capacity. The Shan 1 shale has a relatively high thermal evolution and low organic matter content, restricting organic matter pore development. Clay mineral pores provide specific surface area and adsorption locations for methane, and the intergranular pores of clay minerals are important factors affecting the methane adsorption capacity.

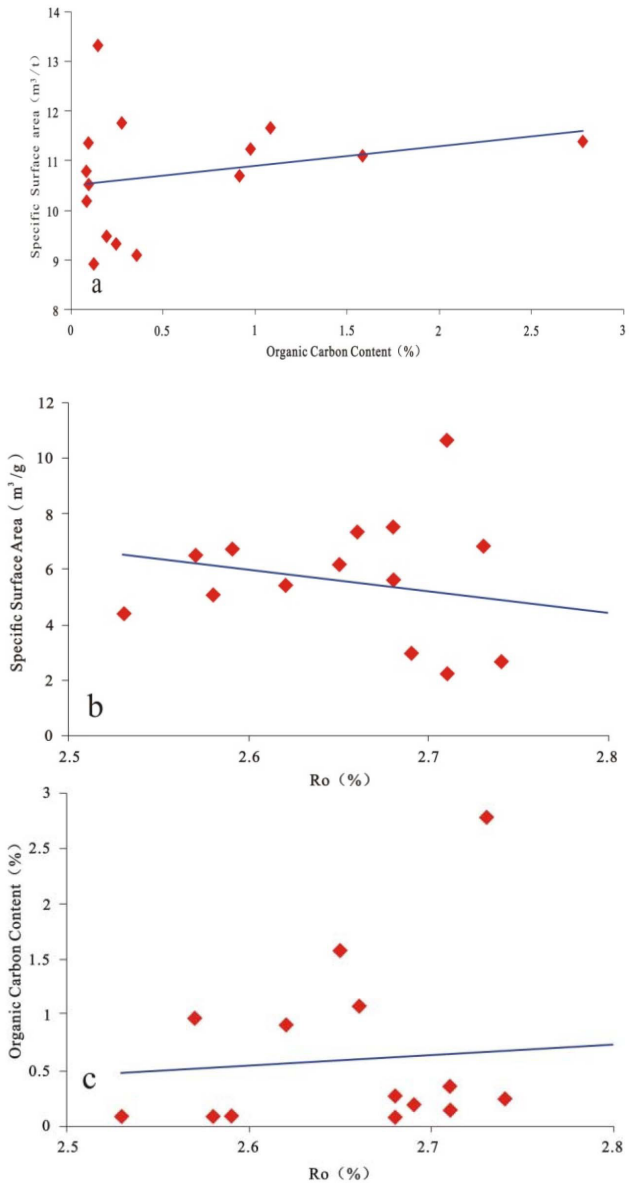

Fig. 13 Relationship between organic carbon and Ro with the adsorption capacity in Shan 1 member shale of well Quan 56 in the Yan'an area.

Declaration of Interest: None

Acknowledgments

This research was jointly supported by the National science and technology major project (2017ZX05039001-002), the National Natural Science Foundation of China (Grant No. 41102083), the Undergraduate Innovation and Entrepreneurship Training Program "Research on pore Characteristics and Influencing Factors of Continental Shale Gas Reservoirs in Ordos Basin" (201910705035).

References

1. Wang, X. Z.; Gao, S. L.; Gao, C. (2014). Geological features of Mesozoic continental shale gas in south of Ordos Basin, NW China, Petroleum Exploration and Development, 41(3), 294-304, doi.org/10.1016/S1876-3804(14)60037-9.
2. Jiang, C. F.; Wang, X. Z.; Zhang, L. X.; Wan, Y. P.; Lei, Y. H.; Sun, J. B.; Guo, C. (2013). Geological characteristics of shale and exploration potential of continental shale gas in 7th member of Yanchang Formation, southeast Ordos Basin. Geology in China,40(6),1880-1888.
3. Zhao, Q. P.; Gao, C.; Yin, J. T.; Zhang, L. X.; Cao, C.; Liu, G.; Yang, X.; Xu, J.; Chen, Y. Y. (2018). Hydrocarbon generation characteristics of source rocks in Shanxi Formation of Xiasiwan Area, Ordos Basin. Journal of Xi'an University of Science and Technology, 38(1),108-117.
4. Zhang, L. X.; Jiang, C. F.; Guo, C. (2012). Exploration potential of Upper Paleozoic shale gas in the eastern Ordos Basin. Journal of Xi'an Shiyou University(Natural Science Edition),27(1),23-26(34), doi.org/10.1260/0144-5987.33.1.
5. Gong, M. L.; Ding, W. L.; Pi, D. D.; Cai, J. J.; Zhang, Y. Q.; Fu, J. L.; Yao, J. L. (2013). Forming conditions of shale gas of the Shanxi Formation of Permian in the southeast of Ordos Basin, Journal of Northeast Petroleum University,37(3),1-10.
6. Fu, J. H.; Guo, S. B.; Lin, X. S.; Wang, Y. G. (2013). Shale gas accumulation condition and exploration potential of the Upper Paleozoic Shanxi Formation in Ordos Basin, Journal of Jilin University (Earth Science Edition),43(2),382-389.
7. Qin, X. L.; Li, R.X.; Wang, X. Z.; Liu, H. Q. (2015). Measuring methods of shale gas content of Shanxi Formation in central and southern Ordos Basin, Natural Gas Geosciences, 26(10): 1984-1991.
8. Lan, C. L.; Guo, W.; Wang, Q.; Zhang, X. (2016). Shale gas accumulation condition and favorable area optimization of the Permian Shanxi Formation, Eastern Ordos Basin, Acta Geologica Sinica, 90(1): 177-188.
9. Zhang, P. H.; Liu, Y. L.; Jia, L. L. (2016). Shale gas reservior characteristics of the Upper Paleozoic coal measures and exploration direction in eastern Ordos basin, Coal Geology & Exploration, 44(4): 54–58.
10. Xi, Z. D.; Tian, Z. B.; Tang, S. H. (2016). Characteristics and main controlling factors of shale gas reservoirs in transitional facies on the eastern margin of Ordos Basin, Geology in China, 43(6): 2059-2069.
11. Feng, Z.Q.; Yu, B. S.; Zeng, Q. N.; Li, Y. F.; Jiang, H. J. (2013). Characteristics and main controlling factors of shale gas reservoir in the Southeastern Ordos Basin, Special Oil and Gas Reservoirs, 20(6): 40-43.
12. Xu, L. F.; Cheng, Y. S.; Zhang, J. C.; Yang, L.; Yang, Y. Y. (2022). Controls on the organic matter accumulation of the marine–continental transitional shanxi formation shale in the Southeastern Ordos Basin, ACS Omega,7(5): 4317-4332.
13. Xu, H. W.; Li, X. Q.; Zhou, B. G.; Qi, S.; Zhang, J. Z.; Yang, J., Chen, J. M.; Gao, W. J. (2017). Characteristics of terrestrial shale gas reservoir in Yanchang exploration area of Ordos basin, Coal Geology & Exploration,45(6): 46–53.
14. Wen, F. G.; Zhu, Y. S.; Ren, Z. L.; Ni, J.; Gao, P. P. (2018).Reservoir porosity characteristics and controls of the Shanxi Formation shale reservoir, Yanchang area, Ordos Basin. Petroleum geology & experiment, 40(6): 778-785.

15. Yang, Y. Y.; Zhang, J. C.; Xu, L. F.; Li, P.; Liu, Y.; Dang, W. (2022). Pore structure and fractal characteristics of deep shale: a case study from permian shanxi formation shale, from the Ordos Basin. ACS Omega, 7(11): 9229-9243.
16. Wang, Z. L.; Guo, S. B. (2019). Pore characterization of shale in Shanxi Formation, Yan'an area, Ordos Basin, Petroleum Geology and Experiment, 41(1): 99-107.
17. Du, Y.; Liu, C.; Gao, C.; Guo, C.; Liu, G.; Xu, J.; Xue, (2020). P. Progress, challenges and prospects of the continental shale gas exploration and development in the Yanchang exploration area of the Ordos Basin, China Petroleum Exploration, 25(2): 33-42.
18. Sun, J. B., Hao S. Y., Zhao, Q. P., Luo, T. Y., Jiang, L., Gao, C., Guo, C., Yin, J. T.; Liu, G. and Xu, J. (2022). Reservoir characteristics and key technologies for shale gas exploration and development of the first member of the Permian Shanxi Formation in Yan'an area, China petroleum exploration, 27(3): 110-120.
19. Guo, S. B.; Zhao, K. Y. (2014). Gas-bearing influential factors and estimation of shale reservoirs in Upper Paleozoic, Ordos Basin, Petroleum geology & experiment, 36(6): 678-683(691).
20. Loucks, R. G.; Reed, R. M.; Ruppel, S. C.; Hammes, (2012). U. Spectrum of pore types and networks in mudrocks and a descriptive classification for matrix-related mudrock pores: AAPG Bulletin, 96(6): 1071-1098.
21. Zhao, B. S., Li, R. X., Qin, X. L., Liu, F. T., Wu, X. L., Zhao, D., Liu, Q. and Zhou, W. (2019). Characteristics of shale reservoirs in the upper paleozoic shanxi formation in the Central Ordos Basin, Acta sedimentologica sinica, 37(6): 1140-1151.
22. Tang, X., Zhang, J. C., Ding, W. L., Yu, B. S., Wang, L., Ma, Y. L., Yang, Y. T., Chen, H. Y. and Huang, H. (2016).The reservoir property of the Upper Paleozoic marine-continental transitional shale and its gas-bearing capacity in the Southeastern Ordos Basin, Earth Science Frontiers, 23(2): 147-157.
23. Groen, J. C.; Peffer, L. A. A.; Pérez-Ramírez, J. (2003). Pore size determination in modified micro-and mesoporous materials, Pitfalls and limitations in gas adsorption data analysis, Microporous and Mesoporous Materials,60, 1-17.
24. Ross, D. J. K.; Bustin, R. M. (2007). Shale gas potential of the lower jurassic gordondale member, Northeastern British Columbia, Canada, Bulletin of Canada Petroleum Geology, 55(1): 51-75.
25. Chalmers G.R.L.; Bustin R.M. Lower. (2008). Cretaceous gas shale in northeastern British Columbia, Part I: Geological controls on methane sorption capacity, Bulletin of Canada Petroleum Geology, 56(1): 1-21.